CHALMERS
UNIVERSITY OF TECHNOLOGY

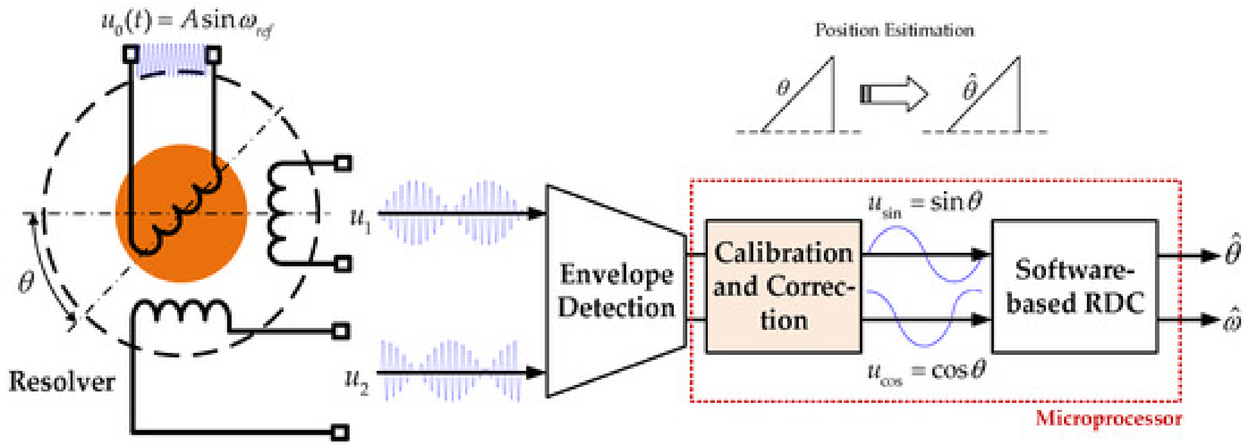

Robust Resolver Signal Acquisition

Master's thesis in *Electric Power Engineering*

Sundar Murugan Ramaswamy
Xiong Xiao

DEPARTMENT OF ELECTRICAL ENGINEERING

CHALMERS UNIVERSITY OF TECHNOLOGY
Göteborg, Sweden 2022
www.chalmers.se

Master's thesis 2022

Robust Resolver Signal Acquisition

Sundar Murugan Ramaswamy
Xiong Xiao

CHALMERS
UNIVERSITY OF TECHNOLOGY

Department of Electrical Engineering
Division of Electric Power Engineering
Chalmers University of Technology
Göteborg, Sweden 2022

Robust Resolver Signal Acquisition
Sundar Murugan Ramaswamy
Xiong Xiao

Supervisor: Joachim Härsjö, Electric Drive Software department, Volvo Cars
Examiner: Torbjörn Thiringer, Professor, Electrical Engineering

Technical Report no.
Department of Electrical Engineering
Division of Electric Power Engineering
Chalmers University of Technology
SE-412 96 Göteborg
Telephone +46 (0)31-772 1000

Cover: Resolver.

Chalmers Bibliotek, Reproservice
Göteborg, Sweden 2022

Robust Resolver Siganl Acquisition
Sundar Murugan Ramaswamy
Xiong Xiao
Department of Electrical Engineering
Division of Electric Power Engineering
Chalmers University of Technology

Abstract

In order to be able to operate electrical devices to create the necessary speed and torque to push the car, inverters are utilized in the automobile industry. Resolver - a very accurate and reliable speed and position sensor is often utilized to have precise control over the electrical equipment that powers the vehicle. The primary goal is to provide a strong signal acquisition of the speed and position from the resolver outputs in a robust manner. Considering the above requirements, fault corrections methods were studied through literatures and models were replicated in Matlab and Simulink for better understanding. Knowing its pros and cons, improvements are made accordingly. The errors with the highest influence on the outputs are treated first followed by the angle tracker. A resolver model is created as part of the effort in order to test and improve the necessary algorithms. In the end, the project concludes with an optimal method for angle encoding.

Index Terms: Resolver, angle, errors, tracker, inverter and Simulink.

Acknowledgements

Throughout the course of our master thesis, Chalmers University of Technology and Volvo Cars Corporation provided continuous assistance and valuable guidance.

Hereby, we would like to thank our professor and examiner Torbjörn Thiringer for sharing his expertise and monitoring our progress. We also like to thank Joachim Härsjö, our supervisor at Volvo Cars Corporation, for giving us the necessary resources and assisting us with his technical knowledge. We are really appreciative and grateful of the academic assistance and opportunities that have been given to us.

Sundar Murugan Ramaswamy and Xiong Xiao
Göteborg, Sweden, Aug 2022

Contents

1
Introduction

As the automotive industry continues to evolve and the regulations of fuel efficiency and emissions, electric vehicles are gradually entering the public eye, including Hybrid Electric Vehicles(HEV), Battery Electric Vehicles(BEV) and Electric Vehicles(EV). More and more electronic components are installed in the cars, one important part among them is called 'Resolver'. The resolver is placed at the rotor of the electric motor which feeds the rotor position at the required frequency for calculating the torque and speed requirements to the inverter. One example of a typical state-of-the-art electric drive train architecture for passenger cars is shown in Figure 1.1.

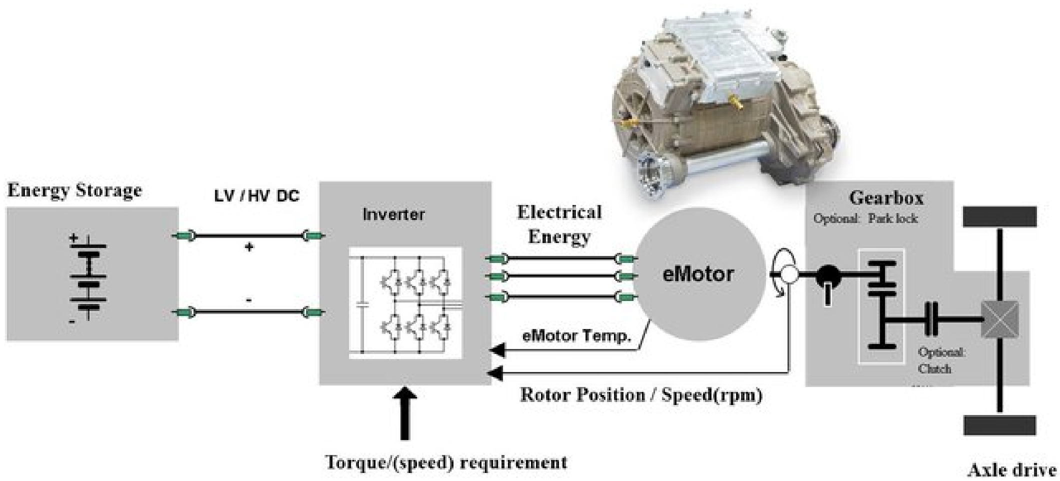

Figure 1.1: Resolver position in an electric powertrain

1.1 Problem background

Resolver is a highly durable and cost-effective angle encoding sensor. In Permanent Magnet Synchronous Motors(PMSM), resolvers are utilized to measure position and speed. Moreover, the purpose of rotor position is to determine where the permanent magnets in the rotor are pointing so that the controller can generate the stator field that attracts the rotor and produces torque/rotation. In order to maintain constant torque generation, the stator field must be adjusted while the rotor moves.

As rotor position is a coordinate reference in PMSM vector control, precise rotor position information is essential. Hall-effect sensors, encoders, resolvers and other devices are used to measure the position of motors. Resolvers, among these sensors, have good endurance in a variety of conditions and can be used in a wide temperature range and more bandwidth.

Resolvers also have the shortcoming of carrying periodic error components in the output voltage. The errors in the resolver are mainly due to mechanical faults or manufacturing defects. In real life, there are not only errors caused by the hardware manufacturing process, but also the influence of external vibration, noise and other disturbances on the sensor which has to be considered. Some signal processing techniques are required to improve angle tracking accuracy of the resolver. It is required to identify the magnetic pole location of the motor and precisely grasp its rotational speed in order to operate the motor in accordance with the varied driving conditions of a vehicle. For these operations, the resolver acts as a sensor. Hence, precise measurement of angle is necessary for continuous operation of the vehicle or else the vehicle will stall as the exact torque required cannot be generated. Hence fault correction algorithms are necessary in order to obtain robust signals from the resolver.

1.2 Goal

This master thesis aims to analyse the shortcomings of the algorithms made use of in the Resolver to Digital Converter(RDC) for encoding the angle of the rotor in different publications and existing literature and develop fault correction algorithms to address those shortcomings. Therefore increasing the robustness of the RDC.

1.3 Previous work

Looking through existing literature, it was evident that the Angle Tracking Observer(ATO) with Proportional Integral Controller(PIC) was highly used to obtain the speed and position of the rotor by processing the signals of the sensor [1][2][3][4]. Hence, an ATO is always needed for angle encoding alongside which our new improvement algorithms can be added.

With an emphasis on position bias fault, amplitude imbalance, and quadrature imperfection, the study [1] conducts an analytical investigation of the resolver fault propagation in electrified powertrain. Based on a mathematical model of a surface-mounted Permanent Magnet Synchronous Motor with direct Field-oriented Control, the defect mechanism is examined. After that, the impact of resolver faults on PMSM drives is examined analytically and statistically. The simulation findings of the resolver fault propagation at the vehicle level over a number of driving cycles are also shown in the article. The outcomes were observed to sufficiently develop a resolver fault diagnostic scheme and provide speed matching requirements for mode transition control in hybrid electric cars.

In order to correct for position inaccuracy, the study [2] suggests an acceleration-compensated ATO that uses its own estimated speed to provide a signal proportional to the motor's acceleration. The ability of the suggested ATO to precisely predict the rotor position of an accelerating motor is first theoretically confirmed. Its stability requirement is also inferred. Second, under two specific conditions, first-order and second-order systems are chosen to approximate the suggested observer, a third-order system, as it is too complex to be directly analyzed. Based on this, a straightforward formula for fine-tuning the suggested ATO is provided, allowing it to maintain the advantages of the traditional one while accurately predicting the rotor position without introducing steady-state inaccuracy. Experiments are then conducted on a resolver installed on a 20 kW permanent magnet synchronous motor. The capacity of the acceleration-compensated ATO to precisely track an accelerating motor's location in compared to that of its conventional version is demonstrated by experimental findings.

The research [3] suggests a brand-new ATO algorithm to correct position inaccuracies brought on by amplitude imbalance. This is simple, straightforward, and economical when using software. Particularly, premeasured offline data are not necessary. It can function as online compensation. The suggested method is put to the test through simulation and experimentation.

In a software-based RDC, ATO with a Phase Locked Loop (PLL) structure, a type II ATO system typically produces steady state errors or cumulative errors despite reducing the noise and controlling the phase error. But type III ATO may offer a remedy. But strong acceleration signals have an impact on them. This study [4] suggests a type IV ATO system with an enhanced PLL that may mitigate strong acceleration signals that occur in a type III ATO. The ATO is then calibrated appropriately for noise suppression and error correction.

However, the authors only process and analyze the occurrence of a single error in most of the literature for fault diagnosis and rectification [3][5][6] and not aggregating all the errors altogether, moreover, also ignoring white noise interference during signal processing, which greatly deviates from the actual situation in real life.

1.4 Purpose

The purpose of this project is to process the errors which has a major influence on the output of the resolver at the same time, and compare the signals obtained under the presence of manufacturing defects and external interference, so that the Resolver to Digital Converter(RDC) can obtain the accurate speed and position information in a very short time by designing different algorithms for comparing the robustness. The output angle is fed into the inverter at a specified frequency.

The goal of the project is to reduce the influence of errors in the signals from resolver, including DC offset, amplitude imbalance, phase shift, imperfect quadrature and noise, and to avoid secondary error, such as delay in the process of the error correction, so that the error between the final obtained position and the actual position is less than 2 degrees. Less than 2 degrees because, the effect of 2 degrees in the output is negligible and does not have quite an effect on the output. reduce the impact of errors

1.5 Scope and limitations

The scope of this thesis project includes,

- Reviewing literatures to examine various techniques utilized in the RDC and comprehend their flaws.

- Simulating those techniques to learn how the RDC's algorithms operate in order to make improvements.

- Adding errors to the resolver model and understanding their shortcomings.

- Making improvements in the above existing methods to improve the robustness of the resolver.

The current issue is that this thesis study only considers RDC simulation, not RDC implementation in hardware.
1) First of all, the simulation time required to run the models is a problem since the resolver sensor must be simulated at high frequency.
2) Further, the values of the errors added to the resolver model is unreasonably high in order to test our algorithm to analyse its behaviour with extremities.
3) Additionally, because of the model's additional uncertainties, the simulation's outcomes are simply accurate approximations that might contain statistical flaws.

1.6 Research questions

The research questions that have been answered as a result of the completion of the thesis are the next to be discussed once the problem statement has been clarified.
1) How will the resolver be simulated given that neither the resolver's model nor the RDC method utilized are provided?
2) Only randomly inserted errors can be added to a resolver. How can the inaccuracies be quantified in that case?
3) Can state estimation techniques be used to strengthen the Resolver to Digital Conversion algorithms?

1.7 Report outline

The report is organized as follows: First, the thesis begins with some background study on the subject by citing articles that had previously studied resolver modeling, Resolver to Digital Converter techniques, error simulations and various state estimation techniques. Following this is the case setup in which the different RDC methods have been replicated from publications to simulation for further study and comparison and thus understanding its shortcomings. Next to this is the analysis part in which the improvements made to the existing models and combining the advantages of the different methods for robustness. The output results and accuracy of the RDC algorithms used earlier are included in the conclusion. It ends with a discussion of potential future work that may be done while keeping in mind the stated topic, which is beyond the scope of this project.

2

Collection of known usable theory

The resolver has simple structure and high stability as a rotary position sensor measuring the speed and the position of the rotor in electric vehicles. This section includes all the theory required to understand about the resolver and its construction and working, RDC, possible errors, fault detection algorithms and signal processing techniques.

2.1 Principle of Resolver

The stator section contains three windings: one excitation winding and two output windings (sine and cosine), the voltage output signals are orthogonally symmetric, that is, sinusoidally and cosinusoidally related to the shaft angle. The resolver's reference winding is in the rotor, while the sine and cosine Windings are in the stator. The sine winding is 90 degrees ahead of the cosine winding in phase. Through electromagnetic induction, the excitation winding is responsible for inducing voltage in the rotor windings. The amplitudes of two-phase voltages from sine and cosine output windings are measured and used to estimate the stator and rotor's relative position when the shaft angle changes. That is, the output from the secondary windings(stator) fluctuates as the primary winding of the rotor rotates. This variation is proportional to the rotor's speed which is then processed by the software based Resolver to Digital Converter(RDC). The schematic of a resolver is shown in figure 2.1

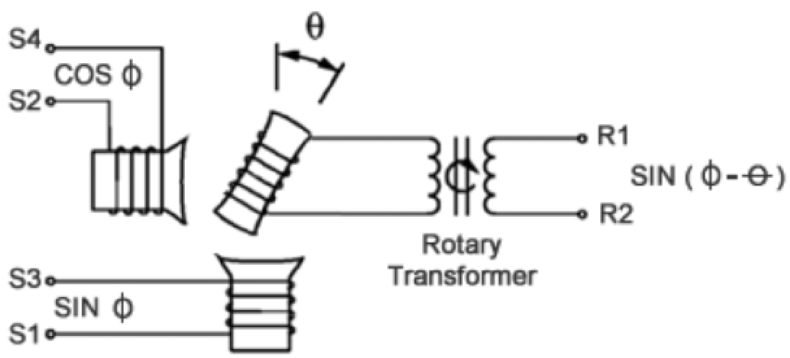

Figure 2.1: Schematic of a Resolver

2.1.1 Electro Magnetic Induction

Electromagnetic induction is a process in which a conductor is placed in a certain position and the magnetic field varies or remains stationary as the conductor moves. A voltage is created across the electrical conductor as a result of this. That is, an alternating current in one conductor produces a changing magnetic field around it. An alternating current can be induced in an adjacent conductor by this magnetic field. The amount of coupling from one conductor to another is determined by the resulting induced voltage as well as the conductors' relative location which is the distance between the rotor and the stator and its geometry.

2.1.2 Transformation Ratio

The transformation ratio is the ratio of the transformer's output voltage to its input voltage. With the location of the resolver rotor, the transformation ratio from the reference winding to the two feedback windings changes [7]. Also due to the resistance in the windings and some leakage flux, there is some loss in voltage. This is called as Voltage Drop. In this project, the value of T_r is chosen as 1 for simplification purposes as voltage drop is not considered.

2.2 Resolver Equations

The software based RDC examines the signal inside the controller or a filter, generating an output that represents the angle the rotor has traveled through, as well as the speed. A high frequency sine carrier signal is fed into the rotor's winding. Under ideal conditions, the excitation signal and the resulting signals at the two output windings are

$$V_e = Asin(\omega_e t) \tag{2.1}$$

$$V_{cos} = T_r V_e cos(\theta_t) \tag{2.2}$$

$$V_{sin} = T_r V_e sin(\theta_t) \tag{2.3}$$

where,
V_e is the excitation winding voltage,
V_{cos} and V_{sin} are the respective cos and sine voltages,
ω_e is the excitation signal's angular frequency and $\omega_e = 2\pi f_r$,
θ_t is the angular position of the rotor,
f_r if the frequency of the carrier signal,
A is the amplitude of the carrier signal,
T_r is the Transmission ratio.

2.3 Resolver to Digital Converter

The output of the resolver needs to be passed into the RDC. The angular position can be estimated using a device called a resolver-to-digital converter based on the resolver outputs. Several RDCs have been suggested in recent years. Hardware-based solutions [8][9][10] and software-based solutions are the two types of techniques [11]. RDC is an external hardware component to the motor controller in hardware-based systems. The scope of this thesis focuses on Software based RDCs. Software based RDCs can be designed in numerous ways. Additionally, in such applications, incremental encoders and resolvers are often utilized mechanical sensors. The majority of RDCs are angle tracking observers or trigonometric observers. Using an appropriate RDC approach, the rotor angle may be retrieved from the demodulated signals. The positioning of the Software based RDC in the resolver model is shown in figure 2.2.

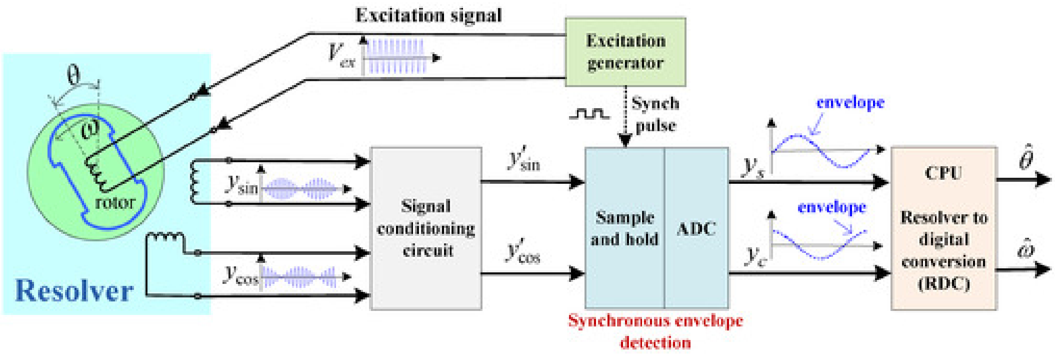

Figure 2.2: Software based Resolver to Digital Conversion(RDC)

2.4 Errors in the signals from resolver

In a realistic system, the resolver signal processing circuits and the resolver itself both produce output signals that contain position inaccuracies. The real resolver output signals as a result have less-than-ideal properties like offset error, scale error, or phase error. Position information can be significantly affected because to the resolver signals' non-ideal properties. Furthermore, noise has a negative impact on effective resolution.

2.4.1 DC offsets

The fit tolerance of the resolver pushed into the rotor shaft when the motor is built determines the resolver offset for each motor. The offset of the resolver has a significant impact on the output characteristics [12]. This DC offset causes the sine and cosine waves to become uneven, that is, the positive and negative peaks are not equidistant from zero. By studying the peaks of the required signal, the dc offset may be determined. The difference in absolute value between each signal's positive and negative peaks is twice its offset. The equations of the resolver outputs with added offset is shown in the below equations.

$$V_{sin} = A\sin(\theta) + A_{os} \tag{2.4}$$

$$V_{cos} = A\cos(\theta) + A_{oc} \tag{2.5}$$

where,
V_{sin} - sin signal received from resolver
V_{cos} - cos signal received from resolver
A is the amplitude of both the resolver output signals,
A_{os} is the DC offset of sine signal,
A_{oc} is the DC offset of cosine signal.

2.4.2 Phase Shift

The two feedback windings on the stator are positioned in quadrature to generate two AC signals that are 90 degrees in phase with each other. Imperfect Quadrature is nothing but the sine and the cosine windings not aligned exactly at right angles to each other. This usually occurs due to manufacturing errors. As a result of imperfect quadrature, phase change between the sine and cosine voltages occur causing phase shift in the signals. This will affect the sampling, so that the sine and cosine signals cannot be sampled when their respective peak values are reached. The resolver output signal with added phase shift term is shown in the below equation.

$$V_{cos} = A\cos(\theta + \beta) \tag{2.6}$$

where β is the phase shift error between sin and cos signals in resolver.

2.4.3 Amplitude imbalance

Although the distance between the two stator windings and the rotor is ideally the same, it is difficult to achieve the same distance in the actual manufacturing process, and errors will occur in the process of magnetic induction transmission, which will cause the amplitudes of the two signals to be different from each other. Also, insulation faults located at the output winding result in an relative amplitude mismatch, or channel mismatch, between the signals.The magnitude of the amplitude imbalance can be described by equations as,

$$V_{sin} = A' \sin(\theta) \tag{2.7}$$

$$V_{cos} = A'(1 + \alpha)\cos(\theta) \tag{2.8}$$

where,
A' is the amplitude for sin signal in resolver,
α is the amplitude imbalance parameter between sin and cos signal.

2.4.4 Noise

The resolver system will be disrupted by a lot of noise in the field. Noise can occur from a variety of sources, including electric motor vibrations, electrical component inference, and other noise sources. This causes different interferences to occur leading to incorrect output readings, and noise will be generated in the acquired signal. Also, the excitation signal distortion causes random noise to arise. But random noise is distributed in all frequency domains. If a low-pass or band-pass filter is used, the interference caused by noise can be reduced to a certain extent, the noise cannot be completely eliminated as the low pass filter(LPF) is employed to eliminate high frequency noise from the signal while maintaining its low frequency components, and the use of a low-pass or a band-pass filter will cause certain delay.

The factors that cause noise in the system are divided into external and internal factors. External influences include sources of noise from other equipment. Internal factors, on the other hand, are sources of noise emanating from Kalman filters, which operate as estimators by taking into account covariance noise, both process and measurement noise [13].

2.5 Sample and Hold

Sampling is the conversion of a continuous-time signal to a discrete-time signal in signal processing. A pulse is provided to the sample and hold (SH) circuits at the positive peak for synchronous demodulation of the amplitude modulated output. Select the sampling frequency of the same frequency as the excitation signal in the sensor, and set the phase delay of one quarter of the sampling time, so that each sampling can obtained at the maximum value of the carrier sin wave so that the signal to noise ratio is the lowest at the peaks. That is, at the rising edge of the excitation signal, sampling and conversion take place using the sample and hold block in SIMULINK. The resolver output signals which has to be demodulated is shown is figure 2.3.

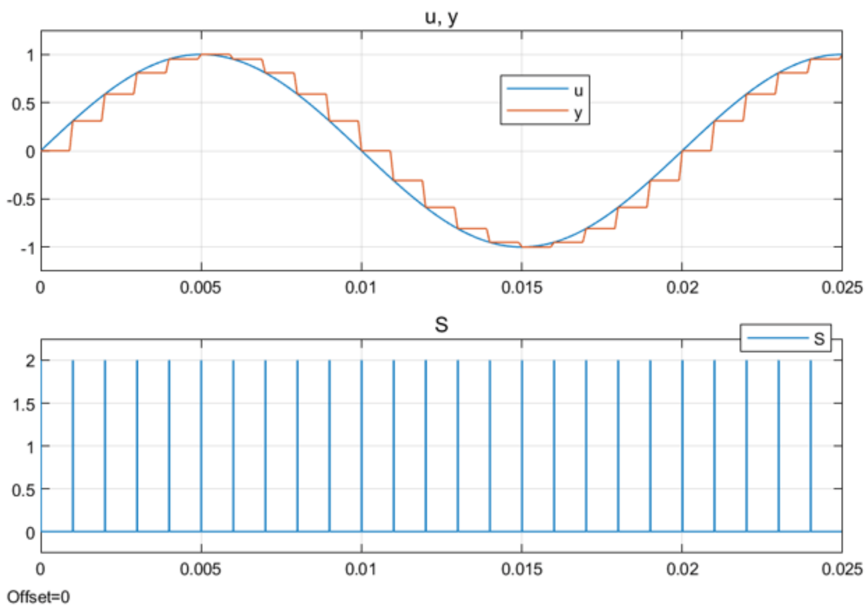

Figure 2.3: Signal discretization

$$V_{sin} = A\sin(\theta) + A_{os} \tag{2.9}$$

$$A\sin(90) + A_{os} = A + A_{os} \tag{2.10}$$

2.6 PI Controller

PIC is the abbreviation of Proportional Integral Controller. Tuning the PIC parameters K_p and K_i, determines the performance of the PI control system. Improper tuning will result in unsatisfactory performance or even instability of the controlled system. PI controller is used instead of PID(Proportional Integral Derivative) controller as we are dealing with noise in the resolver signals because noise when differentiated gets amplified and does not provide the optimum results needed for the software based RDC.

2.7 Control systems

A control system is a collection of devices that controls, commands, directs, or regulates the actions of other devices in order to achieve a certain goal. In other terms, a control system may be defined as a system that directs the actions of other systems to attain a desired state. There are many different types of control systems, which may be divided into linear and non-linear control systems. The next sections go through these different types of control systems in further depth.

2.7.1 Principle of Homogeneity

The principle of homogeneity states that a system which generates an output y(t) for an input x(t) must produce an output ay(t) for an input ax(t).

2.7.2 Superposition Principle

According to the principle of superposition, a system that produces an output $y_1(t)$ for an input $x_1(t)$ and an output $y_2(t)$ for an input $x_2(t)$ must create an output $[y_1(t) + y_2(t)]$ for an input $[x_1(t) + x_2(t)]$.

2.7.3 Linear systems

If a system obeys the principles of homogeneity and superposition, it is said to be linear. As a result, we may claim that a system is linear if the weighted total of its outputs equals the weighted sum of its inputs.

2.7.4 Non linear systems

If a system does not respect the principles of homogeneity and superposition, it is classified as non-linear. A non-linear system is one in which the equation defining the system comprises square or higher order input/output components, or the product of input/output and its derivatives, or a constant.

2.8 Ideal signals from resolver

The resolver output signals of an ideal case which has to be demodulated is shown is figure 2.4

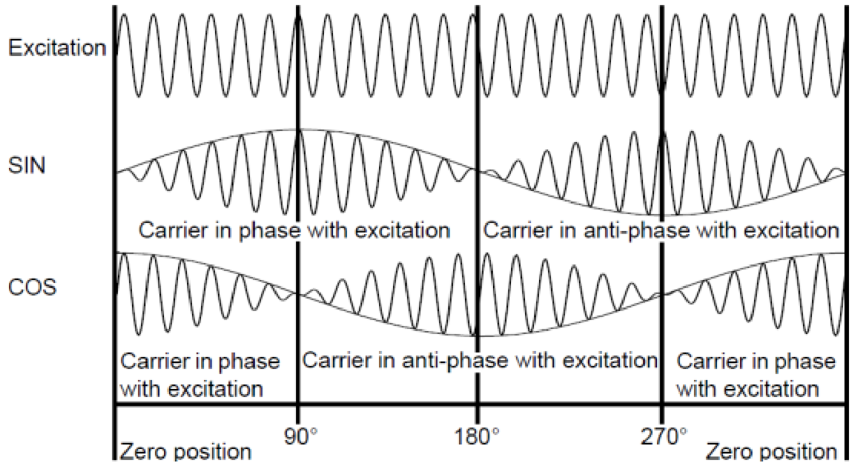

Figure 2.4: Resolver excitation and output signals

2.9 Approaches

Hardware-based approaches are not used in this case to avoid the expenditures of physical pieces, weight and size. The cost of the expensive oscillator and hardware may be avoided by using software-based RDC, and the signals can be demodulated effectively even when the resolver carrier varies widely [14]. As a result, the main element of the various software conversion-based methods for clearing various faults in the output signals from the resolver has been described in the upcoming subsections. The aim of those is to create and compare algorithms that can obtain the signals from the resolver and calculate precise values of the speed and the position of the rotor from the acquired signals. This means the algorithm needs to eliminate the signal errors and noise as much as possible and need short response times.

2.9.1 Arc Tangent Method

The shaft angle is computed using an inverse tangent or the arc tangent function of the quotient of the sampled resolver output voltages V_{sin}, V_{cos} in the trigonometric technique.

$$\theta_t = tan^{-1}(\frac{Asin\theta_t}{Acos\theta_t}) \tag{2.11}$$

The trigonometric approach, on the other hand, just returns data for the unfiltered rotor angle and no information about speed. One more drawback is that a lot of noise is associated with the arc tangent method. As a result, a speed calculation with smoothing capabilities should be included in the final application. The SIMULINK model of resolver to digital converter using the arctangent method is shown in figure 2.5.

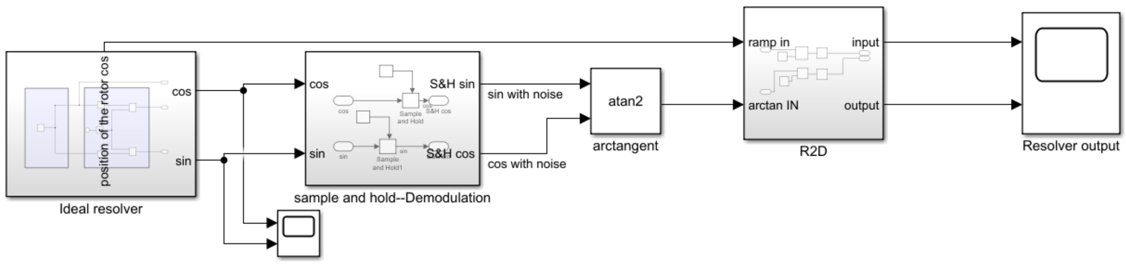

Figure 2.5: SIMULINK model of RDC using arctangent method

2.9.1.1 Ideal arc tangent model

The results from an ideal model of resolver to digital converter using the arc tangent method is shown in figure 2.6. There are no errors and the output values are accurately superimposed on the input values.

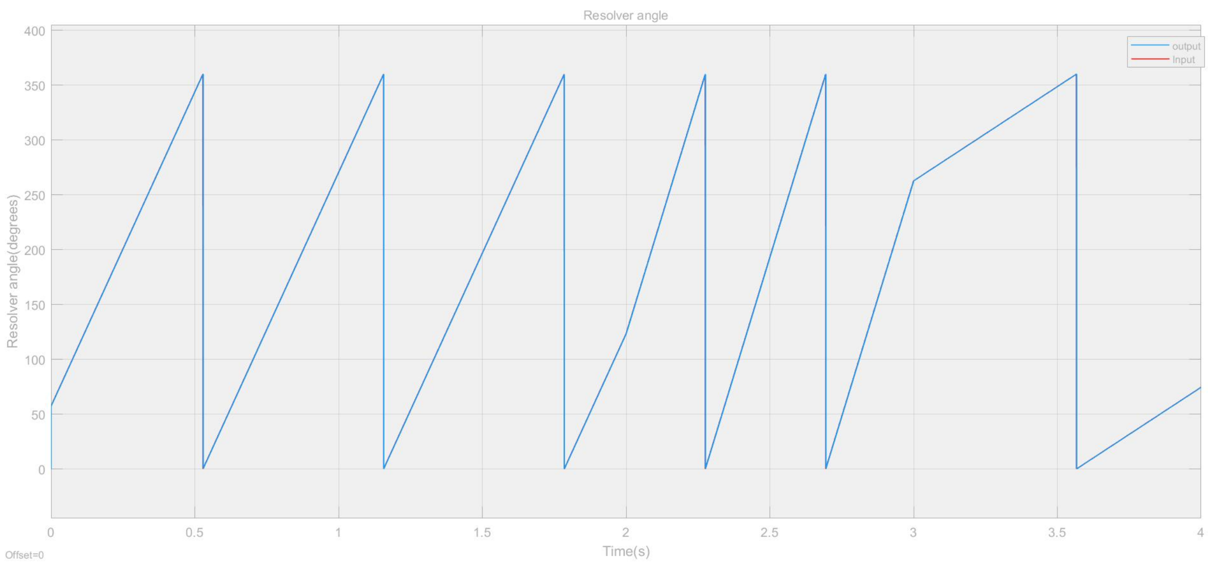

Figure 2.6: Results from RDC using arc tangent method

But the above result is possible only in the ideal case and produces very high errors in the output with the inclusion of errors to the model. If an angle-tracking observer (ATO) is used in an RDC, the flaws occurring in the inverse tangent based RDC can be avoided.

2.9.2 Direct Quadrature transformation

The ATO needs to pass the position error into the PI Controller, and DQ is the method made use of to calculate this error value. Since the estimated value and the actual value should be the same if PIC tracks them correctly, the difference between them is 0. The estimated position is set as θ' and the input measurement as θ, there is a trigonometric function to express as follows,

$$\begin{bmatrix} Q_r \\ D_r \end{bmatrix} = \begin{bmatrix} -\sin\theta' & \cos\theta' \\ \cos\theta' & \sin\theta' \end{bmatrix} \begin{bmatrix} V_{cos} \\ V_{sin} \end{bmatrix} \tag{2.12}$$

in ideal,

$$V_{cos} = A\cos(\theta) \tag{2.13}$$

$$V_{sin} = A\sin(\theta) \tag{2.14}$$

where,
V_{sin} - sin signal received from resolver
V_{cos} - cos signal received from resolver
Expand the calculation formula as follows:

$$Q_r = A(\sin\theta\cos\theta' - \cos\theta\sin\theta') = A\sin(\theta - \theta') \tag{2.15}$$

$$D_r = A(\sin\theta\sin\theta' + \cos\theta\cos\theta') = A\cos(\theta - \theta') \tag{2.16}$$

if A = 1,

$$Q_r = \sin(\theta - \theta') = e \tag{2.17}$$

In this way, the input parameters required by PIC in ATO, is obtained. This inputs the required input parameters to the ATO, which are based on the formula generated by the ideal resolver model.

The actual obtained sin and cos signals contain all the errors mentioned above, and their expressions are:

$$V_{sin} = A'\sin(\theta) + A_{os} \tag{2.18}$$

$$V_{cos} = A'(1+\alpha)\cos(\theta + \beta) + A_{oc} \tag{2.19}$$

where,
A' is the amplitude for sin signal in resolver,
α is the amplitude imbalance parameter between sin and cos signal,
β is the phase error for the signal,
A_{os} is the DC offset of sine signal,
A_{oc} is the DC offset of cosine signal.

Since the value of β is very small in practice, here we assume:

$$
\begin{aligned}
sin(\beta) &= \beta \\
cos(\beta) &= 1
\end{aligned}
\tag{2.20}
$$

The premise of the assumption is that the phase shift angle is small, less than 7 degrees. The equations about Q_r and D_r are expressed as:

$$Q_r = A' \sin(\theta - \theta') - A'\alpha\cos(\theta)\sin(\theta') - A'(1+\alpha)\beta\sin(\theta)\sin(\theta') + A_{os}\cos(\theta') - A_{oc}\sin(\theta') \tag{2.21}$$

$$D_r = A' \cos(\theta - \theta') + A'\alpha\cos(\theta)\cos(\theta') + A'(1+\alpha)\beta\sin(\theta)\cos(\theta') + A_{os}\sin(\theta') + A_{oc}\cos(\theta') \tag{2.22}$$

The difference between position θ and estimate position θ', the value of e for the input ATO should be as small as possible, infinitely approaching 0, so:

$$A' \sin(\theta - \theta') = 0 \tag{2.23}$$

$$A' \cos(\theta - \theta') = A' \tag{2.24}$$

From the above equations, $A' \cos(\theta - \theta')$ is constant, if the formula of D_r is differentiated with respect to θ':

$$\frac{dD_r}{d\hat{\theta}} = A'\alpha\cos(\theta)\sin(\theta') - A'(1+\alpha)\beta\sin(\theta)\sin(\theta') + A_{os}\cos(\theta') - A_{oc}\sin(\theta') \tag{2.25}$$

$$Q_r - \frac{dD_r}{d\hat{\theta}} = A' \sin(\theta - \theta') \tag{2.26}$$

If $A' = 1$:

$$Q_r - \frac{dD_r}{d\hat{\theta}} = \sin(\theta - \theta') = e \tag{2.27}$$

then, the input for PIC in ATO can be obtained.

2.9.3 ATO - Angle Tracking Observer

ATO is the abbreviation of Angle Tracking Observer, which is widely used in situations with unknown speed and position measurement [2][4]. When contrasted to the trigonometric technique, the ATO method has the benefit of smoothly and correctly tracking both the rotor angle and the rotor speed. Various ATO designs have been created so far for various uses [2][4][14][15].

ATO is the combination abut DQ transformation and PI controller. ATO predicts an initial velocity, and then compares the calculated estimated position with the signals from the resolver to obtain the difference, and uses this difference which is the error as an input to the PIC to obtain the speed and position of the rotor. The ATO is a closed-loop system in which the angular position serves as the reference.

Thus, while the motor works at a constant position or speed, a type-II PIC[4] successfully calculates the angular position. The error input to the PIC is shown in the below equation.

$$e = \theta - \theta' \tag{2.28}$$

$$e = \theta - \theta' = \sin(\theta - \theta') = sin\theta cos\theta' - cos\theta sin\theta' \tag{2.29}$$

where,
e - error, the required input to the PIC,
θ - the radian position of rotor, calculated by DQ transformation
θ' - the estimate radian position of rotor, calculated by DQ transformation
$sin\theta$ and $cos\theta$ - received from resolver
$sin\theta'$ and $cos\theta'$ - calculated by using the estimate position obtained in ATO

The difference between position θ and estimate position θ', the value of e for the input ATO should be as small as possible, infinitely approaching 0.

2.10 Bayesian Statistics

Bayesian statistics is a framework for statistical inference. It's a technique for making judgments or drawing conclusions about some parameters of interest utilizing data that has some inherent ambiguity. Bayesian statistics is a method of data analysis based on Bayes' theorem, in which existing knowledge about parameters in a statistical model is updated with new data. To estimate the posterior distribution, background knowledge is described as a prior distribution and paired with observational data in the form of a probability function [16]. A typical example is that the data is imperfect and noisy and does not give us exact information regarding what we are interested in. As a result, Bayesian statistics are used to try to extract as much useful information from our noisy data as feasible. Bayesian statistics is a versatile framework that may be used to a wide range of decisions, including estimation, classification, detection, and model selection. Regardless of the data utilized, the unknown quantities are portrayed as random in Bayesian statistics. That is, the quantities of interest are described as unknown and random. Suppose we wish to estimate a variable θ given measurements y, the key steps in a Bayesian method is as follows.

2.10.1 Modelling

Using a prior or beginning value, we may model what we know about θ and how the measurements y relate to θ. It is the capturing of available knowledge about a given parameter in a statistical model via the prior distribution [16].

2.10.2 Measurement update

To summarize what we know about θ, we combine what we know previously (the prior) with our measurement (also known as the likelihood). It is the process of determining the likelihood function from the parameters provided in the observed data [16].

2.10.3 Decision making

We compute an optimum choice by combining the prior distribution and the likelihood function using Bayes' theorem in the form of the posterior distribution, given what we know about θ and a loss function. The posterior distribution is utilized to make conclusions and represents one's current knowledge by balancing prior information with observed data [16].

2.11 Gaussian distribution

Probability distributions are characterized by their mean vectors and their covariance matrices. The Normal or Gaussian distribution is a bell-shaped curve that is symmetric around the mean and reaches its maximum value of $\frac{1}{\sqrt{2\pi\sigma}}$ which is approximately equal to $\frac{0.399}{\sigma}$ at the mean value of that distribution and σ is the standard deviation. A Gaussian distribution is defined by its mean and its covariance. The centroid of the probability distribution function(pdf) is the mean, or expected value of the variable. The variance is a measure of the random variable's dispersion around the mean [17]. Standard deviation is the square root of the variance. One of the strengths of linear and Gaussian distribution function is that all the densities are Gaussian. The Normal or Gaussian distribution of random variable X is usually represented by the equation below.

$$X \sim \mathcal{N}(\mu, \sigma^2) \tag{2.30}$$

where,
μ is the mean of the normal distribution,
σ^2 is the variance of the normal distribution.

An example for Gaussian distribution with mean 2 and standard deviation 1.5 is shown in the figure 2.7.

The goal of using the Gaussian distribution is to describe the results using the mean vector or expected value and the covariance matrix if the system is linear. Even if our system tends to be non linear, we can still approximate our results using the mean and covariance of this non Gaussian distribution even though all the facets of the actual distribution are not fully captured.

The first practical implementations of Bayesian filtering for continuous spaces were Gaussian filters. Despite a number of drawbacks, they are the most widely used approaches to date.

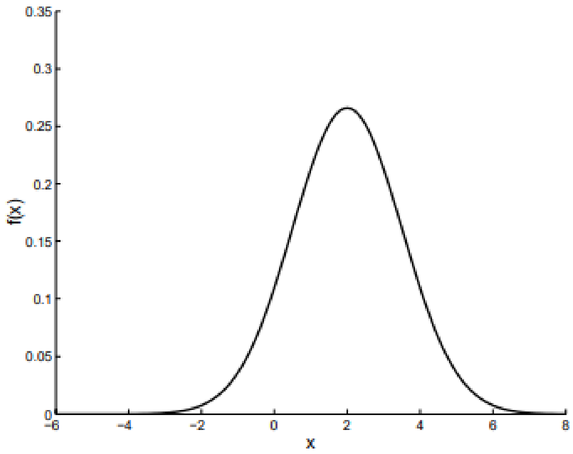

Figure 2.7: Example of a Gaussian or normal probability density function

2.12 The Kalman filter

The kalman filter was developed as a filtering and prediction mechanism for linear Gaussian systems. The kalman filter is a sort of estimator that is efficient at managing noise. As the noise overlapping the input signals from the resolver is significant, an appropriate filter is required. The study proposes a solution to such a problem using a kalman filter properly positioned in a phase locked loop framework. As our problem involves state estimation kalman filter is a suitable option. Moreover, the current trend in motor control is eliminating the usage of sensors and making use of estimating methods for position measurement in automotive applications [6]. Additionally, The KF method estimates the rotor position in addition to the rotor speed. One major reason for moving towards sensorless control is to reduce the cost involved [6]. The kalman filter is frequently used in robotics, navigation, and vehicle control systems, among other applications fro state estimation purposes.

The computation of these the two moments(mean and covariance) are only needed in each step in order to compute the predicted density in the prediction step and the posterior update density in the update step of the kalman filter.

2.12.1 The Extended Kalman filter

The Extended Kalman Filter(EKF) theory is made use of to create an algorithm that is highly efficient and lends itself to straight forward implementation on a digital signal processor or the hardware itself. The method estimates the rotor angle in addition to the rotor speed. The Extended Kalman filter approximates the non-linearities by utilizing a first-order Taylor expansion around the current estimate, followed by the time and measurement update formulas from the filter. Because, in actuality, state transitions and measurements are rarely linear. As a result, it's better to be able to use the filter to simulate non-linear changes. As the system is non linear system which contains errors and does not fllow a specific trend, the EKF will be a suitable option.

2.12.2 Kalman Filtering process and equations

The kalman filter gives the analytical solutions to the filtering equations in linear and gaussian models. The basics of Kalman filter theory are discussed [18]. The Extended kalman filter has been setup using the matlab function block in SIMULINK. The equations are written in the matlab function block and the quantized and demodulated input sine and cosine signals are passed into the block. Any linear dynamic system with discrete time may be expressed in state-space form [6]. A linear system must be used to model the process or system being measured. The following two state space representations in the following equations best explain a linear system.

$$x(k+1) = Ax(k) + Bu(k) - w(k) \tag{2.31}$$

$$y(k) = Cx(k) + V(k) \tag{2.32}$$

where,
The input and output signals are denoted by u(k) and y(k), respectively,
x(k) is the so-called state vector,
The motion noise and measurement noise are denoted by w(k) and v(k), respectively,
A,B, and C are system matrices that can be time-varying in the general case.

The kalman filter recursively computes the mean and covariance of the distribution which are represented by the following equations as,
Prediction step:

$$p(x_k|y_{1:k-1}) = \mathcal{N}(x_k; \hat{x}_{k|k-1}, P_{k|k-1}) \tag{2.33}$$

Update step:

$$p(x_k|y_{1:k}) = \mathcal{N}(x_k; \hat{x}_{k|k}, P_{k|k}) \tag{2.34}$$

where,
k = 1,2,..., representing the time steps,
$\mathcal{N}$ represents the Gaussian distribution,
x_k represents the state variables which are taken into consideration for modelling the system,
$p(x_k|y_{1:k-1})$ is the predicted density which is the distribution of x_k up to time k-1 and computes it as a Gaussian density with mean $\hat{x}_{k|k-1}$ and covariance $P_{k|k-1}$,
$p(x_k|y_{1:k})$ is the posterior updated density which is the distribution of x_k up to time k and computes it as a Gaussian density with mean $\hat{x}_{k|k}$ and covariance $P_{k|k}$.

In equations (2.33 and 2.34), $\hat{x}_{k|k-1}$, $P_{k|k-1}$, $\hat{x}_{k|k}$ and $P_{k|k}$ has to be computed in each recursion.

2.12.2.1 The prediction step

The mean and covariance of the prediction step can be calculated by using the equations as follows.

Predicted mean:

$$\hat{x}_{k|k-1} = A_{k-1}\hat{x}_{k-1|k-1} \tag{2.35}$$

Predicted covariance:

$$P_{k|k-1} = A_{k-1}P_{k-1|k-1}A_{k-1}^{T} + Q_{k-1} \tag{2.36}$$

where,
A_{k-1} is the transition matrix $\hat{x}_{k-1|k-1}$ is the mean of the posterior density from the previous time instance,
$P_{k-1|k-1}$ is the covariance of the posterior density from the previous time instance,
q_{k-1} is the process noise and it is assumed to be zero mean Gaussian with covariance Q_{k-1}.

Thus, we get the predicted mean by simply translating the posterior mean from the previous time instants by multiplying with the transition matrix. The predicted covariance can be derived in a similar manner. Here the posterior covariance is translated by the transition matrix A_{k-1} added with the covariance of the process noise Q_{k-1}.

2.12.2.2 The update step

The mean and covariance of the update step can be calculated by using the equations as follows.

Updated mean:

$$\hat{x}_{k|k} = \hat{x}_{k|k-1} + K_k V_k \tag{2.37}$$

Updated covariance:

$$P_{k|k} = P_{k|k-1} - K_k S_k K_k^{T} \tag{2.38}$$

where,
$\hat{x}_{k|k}$ is the updates posterior mean,
$P_{k|k}$ is the posterior updated covariance,
K_k is the kalman gain,
V_k is the innovation,
S_k is the innovation covariance.

In the update step, we want to correct the predicted estimate with the information from the current observation. The updated posterior mean is calculated by modifying the predicted mean which will act as the prior value added with a correction term as an update. Prior value is the old information that is obtained from the previous measurements and the correction term is the new information that is acquired from the current observation. Similarly, the posterior updated covariance is calculated by using the predicted covariance and shrinking it by a correction factor. In order to calculate the posterior mean and covariance, the kalman gain, innovation and the innovation covariance are calculated by using the following equations.

Kalman gain:

$$K_k = P_{k|k-1} - H_k^T S_k^{-1} \tag{2.39}$$

Innovation:

$$V_k = y_k - H_k x_{k|k-1} \tag{2.40}$$

Innovation covariance:

$$S_k = H_k P_{k|k-1} H_k^T + R_k \tag{2.41}$$

where,
H_k is the y_k is the measurement data obtained from the sensor,
R_k is the measurement noise
From the mean equation, we can infer that only the posterior mean is dependent on the data from the innovation term. Hence we can conclude that only the kalman filter estimate is a function of data and not the uncertainty in our estimates.

If the associated models are linear and the noise is additive Gaussian, the kalman filter is a minimal variance estimator. However, nonlinear dynamic models and/or measurement models are a regular occurrence. The extended kalman filter approximates these non-linearities by utilizing a first-order Taylor expansion around the current estimate, followed by the kalman filter's time and measurement update algorithms [19].

3
Case set-up

This chapter explains how the model of the resolver has been set up in SIMULINK, how it works with the different imbalances, how the errors are setup and results of different RDC designs including similar RDC designs proposed in different publications and their disadvantages.

3.1 Inclusion of errors in resolver model

The block showing the setting of different errors in the SIMULINK model of the resolver is shown in figure 3.1.

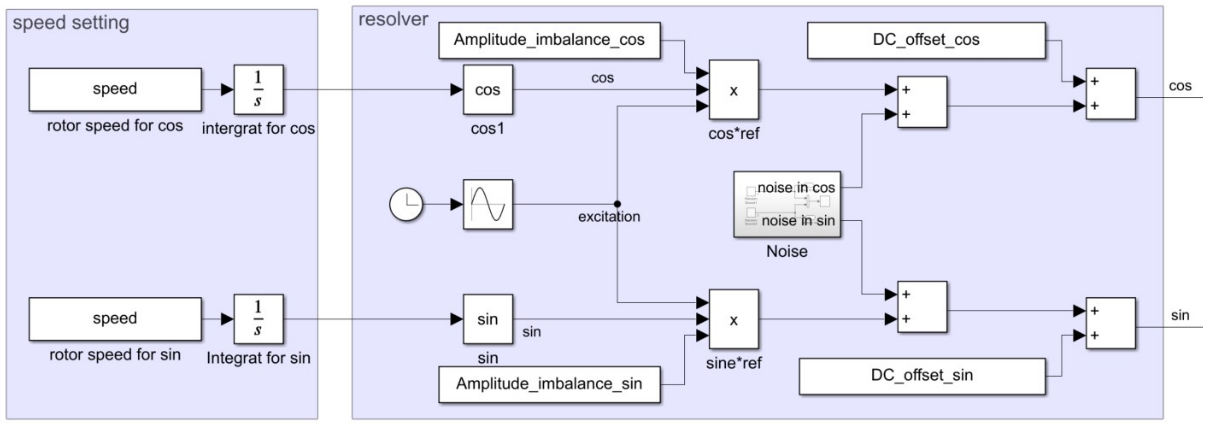

Figure 3.1: Block diagram of the resolver with added errors

The SIMULINK model of the resolver is setup with values of speed and then the integral of the speed is used to input the position. The resolver signals has to be modulated with a carrier frequency. The process of encoding information from a message source in a form that can be sent is known as modulation. Video, speech, and other data can be communicated by superimposing a message over a high frequency signal known as a carrier wave. The excitation signal is often designed to reduce noise while calculating the most accurate frequency response function in the shortest time possible. In this case, the cosine and sine components are then multiplied with the carrier frequency which is a sine wave of frequency 10KHz which is assumed to be ideal for a resolver. Amplitude imbalance, DC offset and phase shift is also included alongside with noise to the model based on our mathematical equations of a resolver presented in the earlier sections. An example for ideal resolver signals and the resolver signals with the included errors are shown in figure 3.2.

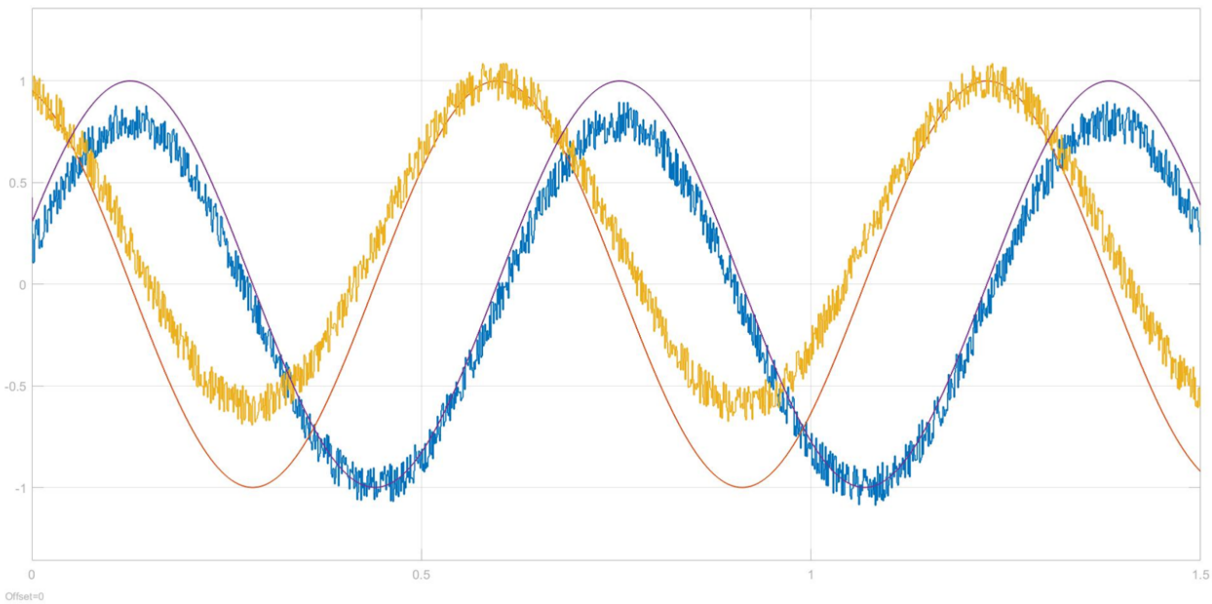

Figure 3.2: Resolver input signals with added errors

3.2 Noise Removal using low pass filter

For a signal doped with noise, a low-pass filter is used to filter the noise. According to Fourier theory, the signal can be regarded as a combination of signals of different frequencies and amplitudes. Therefore, a low-pass filter is used to denoise the collected signal. At the same time, the low-pass filter must not affect sin and cos waves, the frequencies of sin and cos waves depend on the speed of rotor. The number of revolutions the rotor completes per second is the frequency of the output signals in resolver. At present, the speed of the motor used in electric vehicles is close to 15,000 rpm, so the cut-off frequency of the low-pass filter must be greater than 15,000/60 Hz.

3.3 Low pass filter in arc tangent method

A first order butterworth lowpass filter is made use of in this case. The passband is maximally flat, which is a benefit of a Butterworth low pass filter. This indicates a smooth, monotonically declining frequency response in the filter's passband. This sort of filter also has the benefit that choosing a higher order filter will result in a steeper attenuation slope towards the cut-off frequency each time the order of the filter is raised. However, adding more components to the circuit is a drawback of raising the order of the filter and thus increasing computational power. The delayed response of the roll-off between the passband and stopband is another drawback of using a Butterworth filter. The Simulink model of the lowpass filter used alongside the arc tangent is shown in figure 3.3

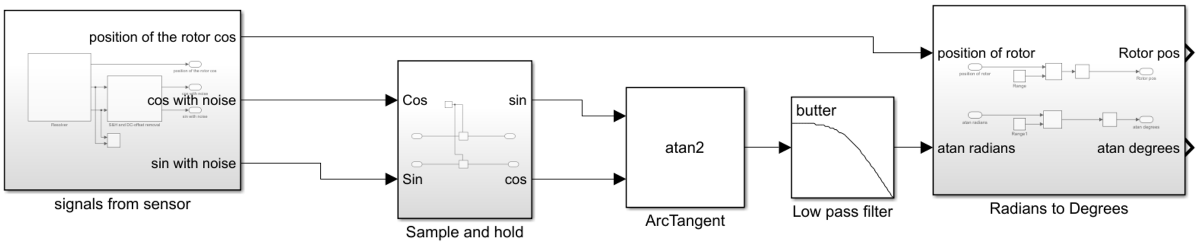

Figure 3.3: Simulink model of arc tangent with butterworth lowpass filter

3.3.1 Results of Low pass filter in arc tangent method

The results shown in figure 3.4 clearly depict the presence of spikes in the ramp at 180 degrees and a lot of noise associated with the output indicated by the spikes throughout the ramp. The error in the output is also close to 5 degrees with a sudden rise to 180 degrees and back in between which is not suitable for a sensor like resolver which requires higher accuracy for safe operation of the electric drive.

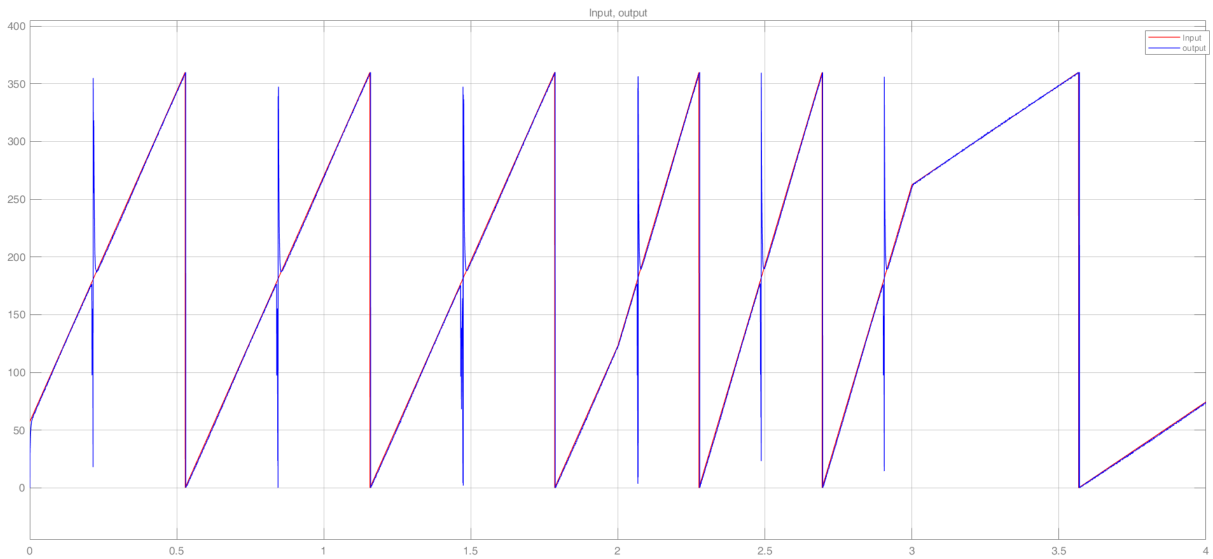

Figure 3.4: Results of RDC based on arc tangent method with butterworth lowpass filter

3.4 ATO model

The ATO settings influence the angle estimation's transient responsiveness. As a result, calibrating the ATO is a critical step in obtaining an accurate and reliable angle estimation. The ATO is setup at the output of the sample and hold block. The input after discretization is multiplied with the feedback as per equation (2.29). The proportional and integral constants are set by trial and error method. This output is then integrated for the position. The Simulink model of ATO is shown in figure 3.5.

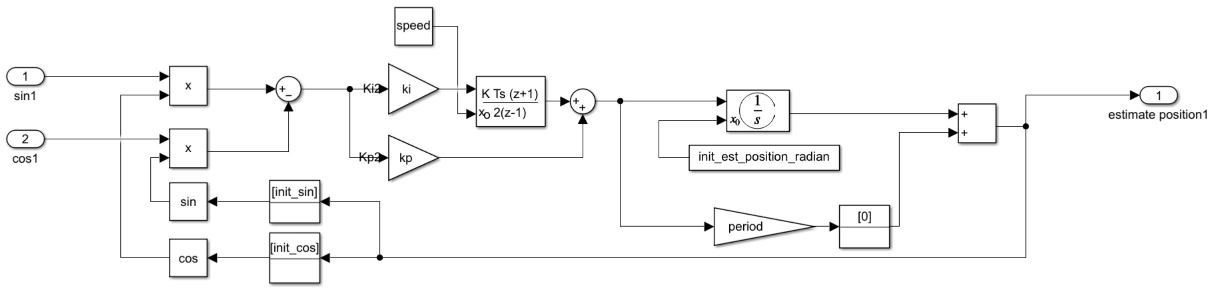

Figure 3.5: Simulink model of ATO

The results of the ATO are shown in the figure 3.6. From the results, it is inferred that the results of the Angle Tracking Observer has errors upto 12 degrees initially and during transitions. Also the time taken by the ATO to converge is around 0.2 seconds. During transitions, the time taken by the ATO to converge to the correct value is around 0.5 seconds in our case which is very high in resolver applications as the tracked value of angle has to be fed into the resolver at a frequency of 10KHz.

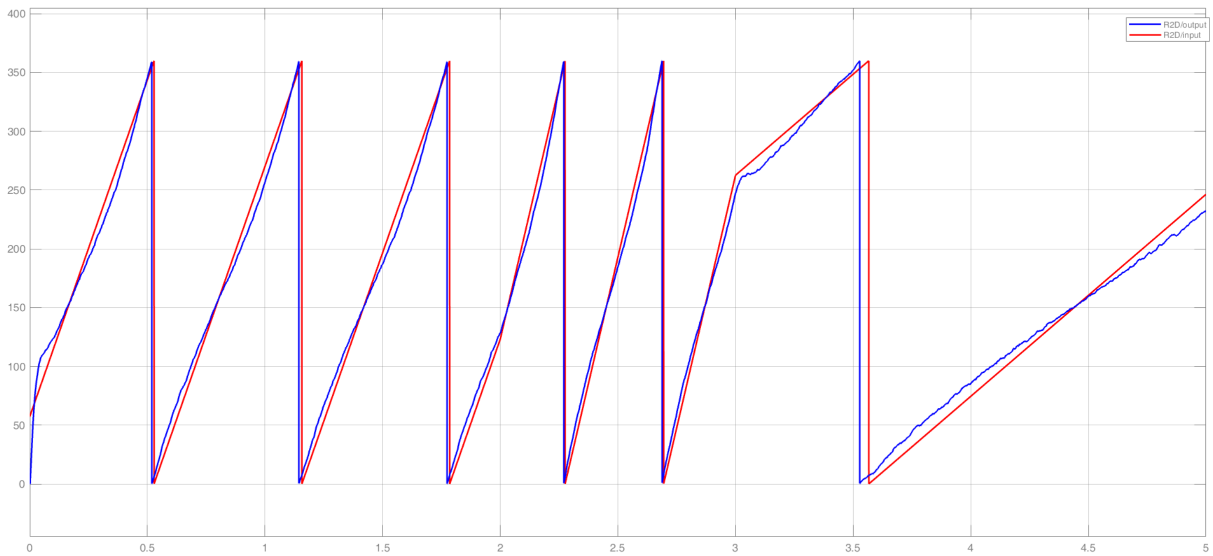

Figure 3.6: Results of Angle Tracking Observer based RDC

3.5 Results of ATO with DQ transformation

From the equations (2.21, 2.22, 2.25 and 2.27), all errors can be easily filtered out through the DQ transformation method, if the amplitude of sin signal in resolver can be obtained and the noise can be filtered out.

In fact, using a low-pass filter is not a good solution to clean the noise. The low-pass filter will cause delay problems, which will further influence the calculation of the speed and position. The white noise will be in each frequency band and the low-pass filter can only filter out the signals with frequency higher than the cut-off frequency, and cannot remove all the noise which is usually random and of any frequency.

If the band-pass filter is used, as the speed of the vehicle is not constant throughout the driving process. According to the motor speed range, 0-20000 rpm, the output signal frequency of the resolver will be maintained between 0-20000/60 Hz, which makes it difficult to use a band-pass filter, even if a low-pass filter is used, the cutoff frequency must be greater than 20000/60 , which allows the filter to remove all noise.

At the same time, when using DQ transformation to clean up errors, D_r cannot be directly differentiated by θ , the relationship between the two is not clear, but a certain transformation can be made. The D_r formula needs to be differentiated as given in the equation.

$$\frac{dD_r}{d\phi} = \frac{dD_r}{dt}\frac{dt}{d\phi} \tag{3.1}$$

As a result of this differentiation, the angular velocity of the rotor is required. So the equation becomes,

$$\frac{dD_r}{dt}\frac{dt}{d\phi} = \frac{dD_r}{dt}\frac{dt}{d\omega t} = \frac{dD_r}{dt}/\omega \tag{3.2}$$

Where,
ω is the speed of the rotor in radians.

However, the effect of noise still needs to be considered, the existence of noise will cause the result of the differential equation to have a deterioration in the accuracy of the measurements. Under ideal conditions, with no noise, using DQ transformation and the calculation of dD_r and Q_r can perfectly solve all the other errors, but with noise, the result becomes unstable as the noise gets differentiated.

In order to find the amplitude of the sine signal, it can be obtained by obtaining the peak value of the sine signal, which also means that the amplitude of the sine signal can only be determined after a complete cycle of the sine signal is completed, and the effectiveness is affected. And because of the noise, the resultant peak value is not steady, which also makes it difficult to successfully apply the DQ transformation and perform associated computations. The results obtained from the RDC with ATO and DQ transformation can be seen in figure 3.7. The random spikes are formed as the noise in the system is being differentiated and hence the DQ transformation is not an optimal method for the RDC.

3.6 Results of Kalman Filtering

The kalman filter is designed and setup using the equations (2.31-2.41). The values for the matrices needed for the KF prediction and update steps are as follows.

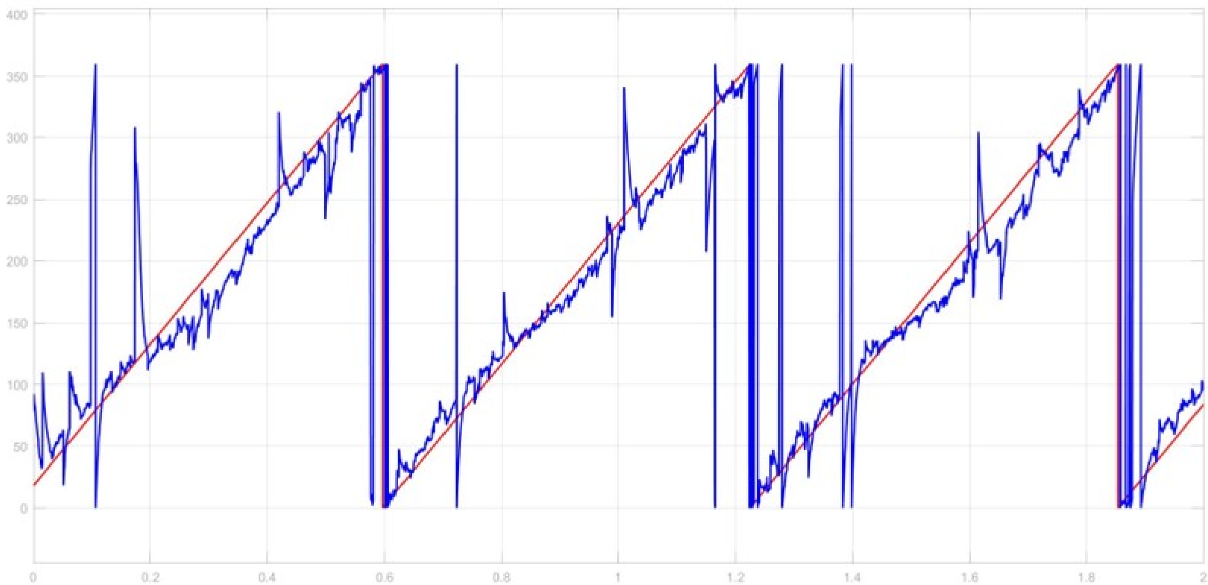

Figure 3.7: Results from RDC with ATO and DQ transformation

$$A = \begin{bmatrix} 1 & T & 0 \\ 0 & 1 & 1 \\ 0 & 0 & 1 \end{bmatrix}, B = 0, C = \begin{bmatrix} 0 & 0 & 0 \\ 1 & 0 & 0 \end{bmatrix}, D = 0$$

$$\hat{x}_{k|k-1} = \begin{bmatrix} 0 & 0 & 0 \end{bmatrix} \text{ (initial mean)}$$

$$\hat{P}_{k|k-1} = \begin{bmatrix} 20 & 0 & 0 \\ 0 & 20 & 0 \\ 0 & 0 & 20 \end{bmatrix} \text{ (initial variance)}$$

$$y_k = \begin{bmatrix} cosIN \\ sinIN \end{bmatrix}$$

$$H_k = \begin{bmatrix} -sin(\hat{x}_{k|k-1}) & 0 & 0 \\ cos(\hat{x}_{k|k-1}) & 0 & 0 \end{bmatrix}$$

$$Q_k = \begin{bmatrix} \gamma 1 & 0 & 0 \\ 0 & \gamma 2 & 0 \\ 0 & 0 & \gamma 3 \end{bmatrix}$$

$$R_k = \begin{bmatrix} \lambda 1 & 0 \\ 0 & \lambda 2 \end{bmatrix}$$

where, T is the sampling period,
cosIN and sinIN are the input signals from the sample and hold block of the resolver model,
$\gamma 1$,$\gamma 2$ and $\gamma 3$ are the values needed to be tuned in the process noise matrix,
$\lambda 1$ and $\lambda 2$ are the values needed to be tuned in the measurement noise matrix.

The initial mean and covariance matrices are 3 by 1 and 3 by 3 matrices respectively as each of the three rows represent position, velocity and acceleration respectively.

The initial values are assigned randomly as the kalman filter has the ability to converge very quick however absurd the mean and variance can be. Those values are assigned to the kalman filter via the unit delay block in Simulink. The values of $\gamma 1$,$\gamma 2$ and $\gamma 3$ are tuned to be 0, 0 and 1 respectively and the values of $\lambda 1$ and $\lambda 2$ are set to 9 and 11 respectively for best possible accuracy of the resolver model.

The kalman filter has been designed using the matlab function block and it is added to the output of the sample and hold. The kalman filter matrix values are set by trial and error method by changing the diagonal values of the motion and measurement noise matrices. The tuning of the kalman filter was found to be simpler compared to the ATO constants through experience. The Simulink model of the kalman filter is shown in figure 3.8.

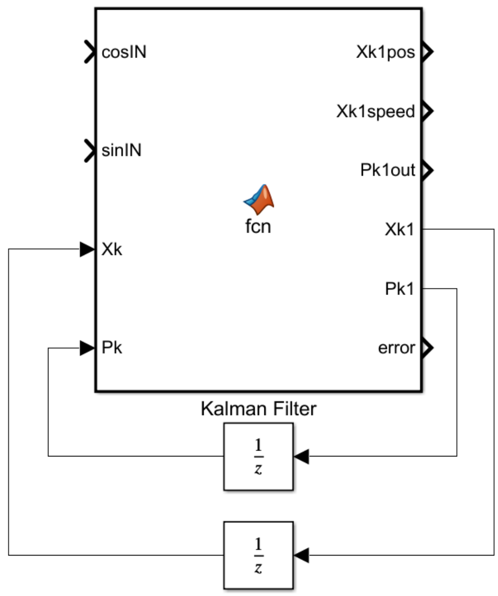

Figure 3.8: Simulink model of a kalman filter based RDC

Sensorless control, enabled by digital signal processors, lowers total system running costs by removing mechanical sensors while maintaining control system functionality. However, sensor less control cannot provide the needed precision and reliability in some situations, particularly in terms of angular position and speed. Due to high speed and acceleration, simulation findings reveal that the outputs of an Extended Kalman Filter can be unreliable. The output of the kalman filter based RDC is shown in figure 3.9.

From the results, it can be clearly seen than the output is not accurately superimposed with the input. The error in the output is upto 12 degrees and not reliable for resolver application. As we can see, initially, the time taken for converging and transitions is quick by the kalman filter compared to the ATO as the KF works based on prediction and update.

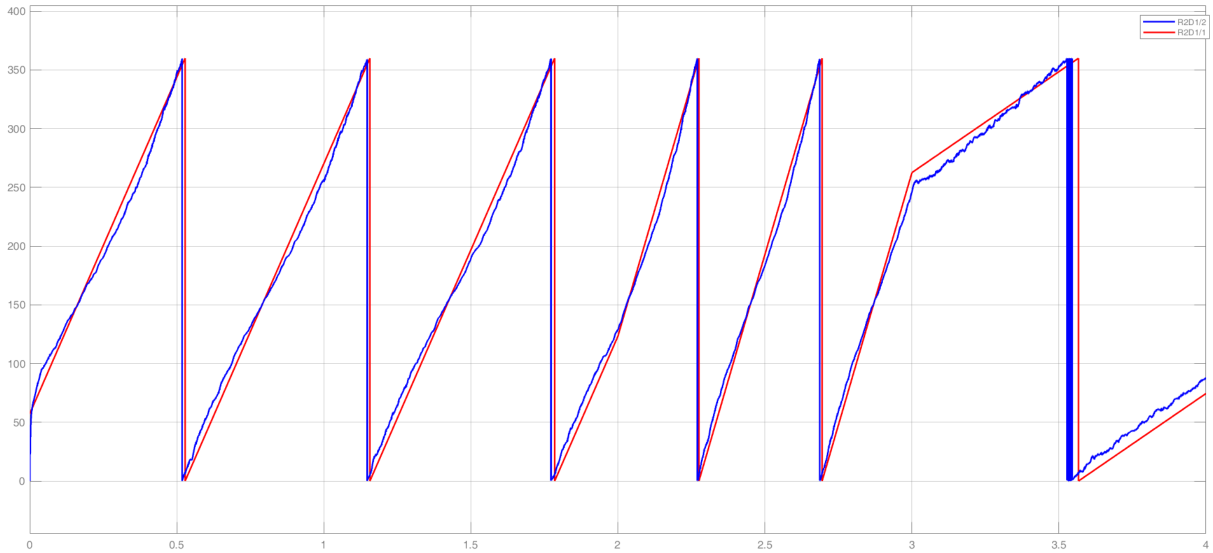

Figure 3.9: Results of the kalman filter based RDC

4

Analysis

This chapter discusses the changes made to the RDC algorithm in light of the issues that were repeated in the earlier parts. The simulation results and the implementation of the suggested RDC system in Simulink are shown.

4.1 Improvement for ATO

The ATO is a good tool for predicting the position. But the ATO itself cannot handle all of the errors to provide a reliable result and hence removing some of the errors before inputting the signal into the ATO was considered. Amongst the errors we are dealing with, DC offset and amplitude imbalance were found to have the highest influence of the output results. Hence, removing the DC offset and amplitude imbalance before tracking the angle could be a solution. That is, by modifying the input signal, the error of the input signal to the ATO can be made smaller, so as to obtain better prediction results.

4.1.1 Double sample and hold

During the simulation experiment, it is found that kalman filter can reduce the impact of phase shift, amplitude imbalance and noise on the signals, but the effect on DC offset is relatively poor, which leads to a high influence on the final prediction results.

Due to the existence of DC offset, the peak values of the sine signal and the cosine signal will be affected. While using the sample and hold function, the maximum value of the sine signal and the cosine signal should be obtained to acquire the discrete signal required as input to the ATO algorithm.

When using 'Double sample and hold' to quantize the input signal, the maximum and minimum values of the sine signal and the cosine signal are captured at the same time, and those signals can be obtained by using equation the below equation.

$$V_{sinmax} = A\sin(90) + A_{os} = A + A_{os} \tag{4.1}$$

$$V_{sinmin} = A\sin(270) + A_{os} = -A + A_{os} \tag{4.2}$$

$$\begin{aligned} (V_{sinmax} + V_{sinmin})/2 &= A_{os} \\ (V_{cosmax} + V_{cosmin})/2 &= A_{oc} \end{aligned} \tag{4.3}$$

where,
V_{sinmax} and V_{sinmin} are the sampled values of maximum and minimum in every excitation signal cycle of the sine signal,
V_{cosmax} and V_{cosmin} are the sampled values of maximum and minimum in every excitation signal cycle of the cosine signal,

The changing of cosine and sine signals are showed in the figure 4.1. The values of offset in signals go back to 0.

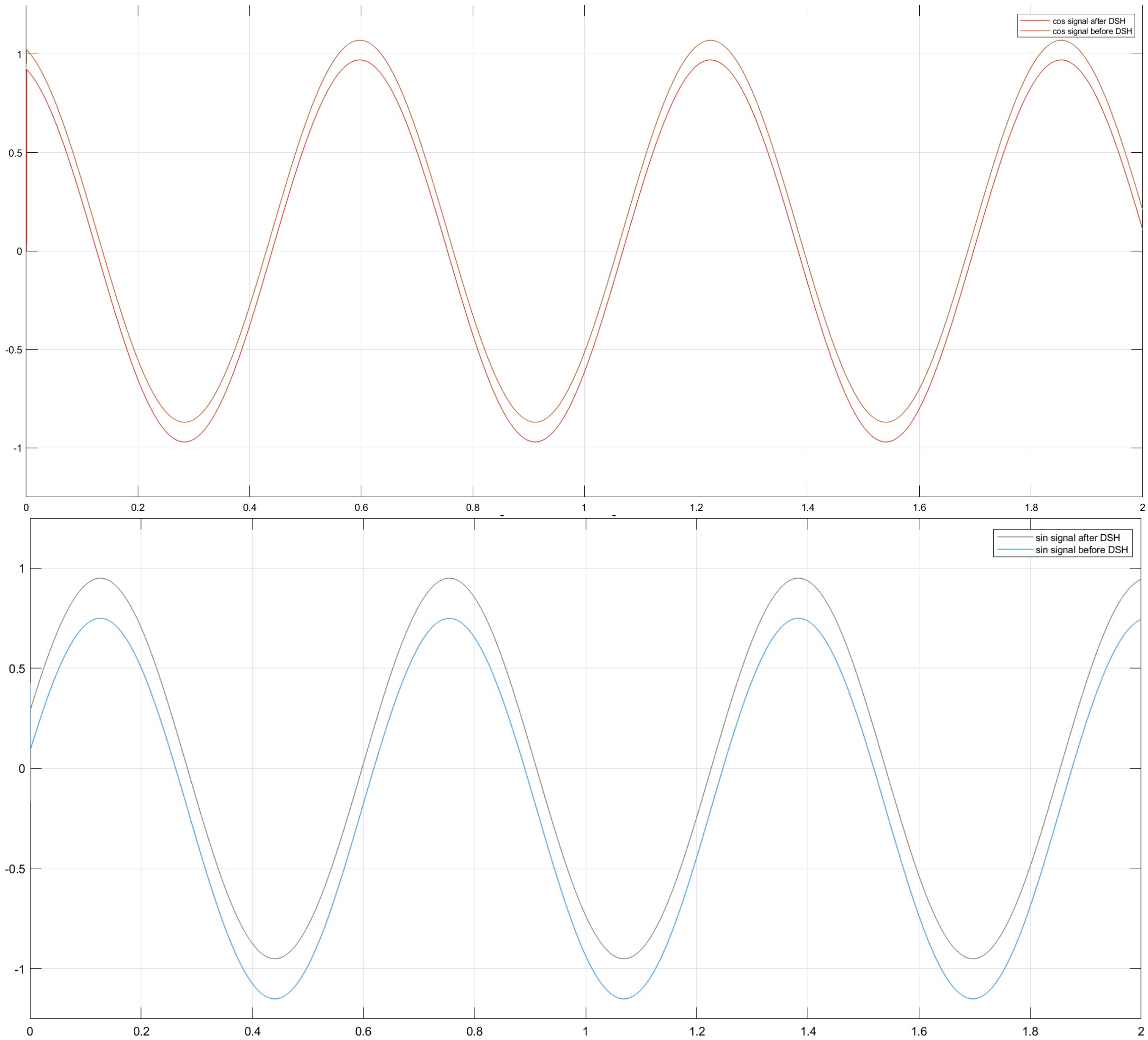

Figure 4.1: Sine/Cosine signals before/after being fixed by double Sample and Hold method

However, it should be noted that since the motor is working and the rotor is rotating when the maximum and minimum values of each cycle in the signal are obtained and the rotor must make one revolution in order to get these two values but the maximum and minimum values are not the parts of the sine and cosine signal with the same amplitude, So the result obtained by Double samplehold is not a fixed value.

When the rotor rotates at high speed, the Double SampleHold method generates an additional high frequency signal in the signal, the frequency of this signal is twice the frequency of the excitation signal.
When the sample and hold frequency is 10,000Hz and the rotor's speed reaches a maximum of 15,000 rpm, a 4.5 degree error in the rotor position occurs. Also, the max amplitude change recorded is 0.079.

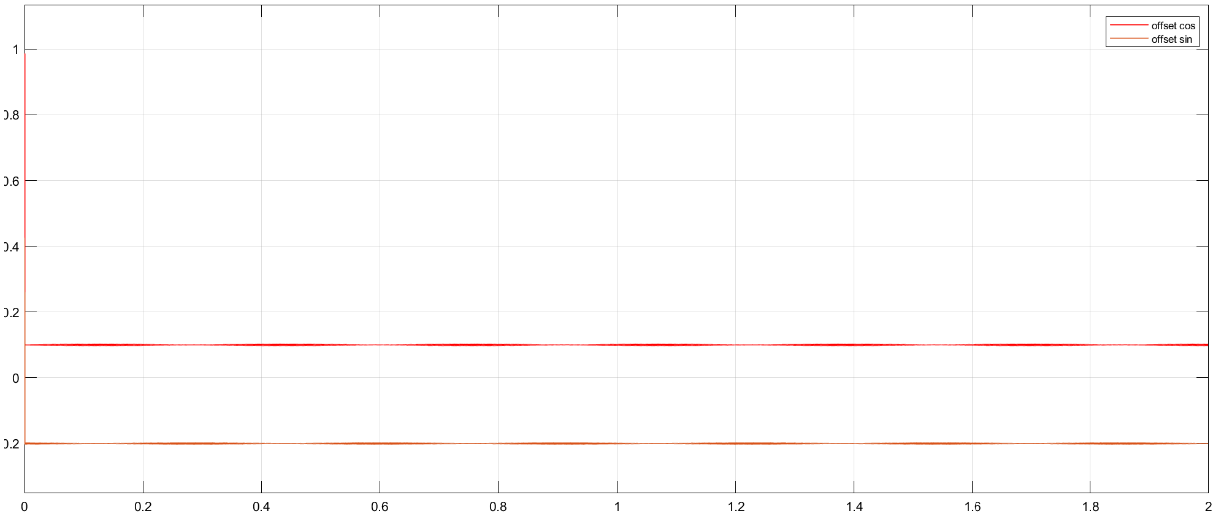

Figure 4.2: Offset of the sine and cosine signals

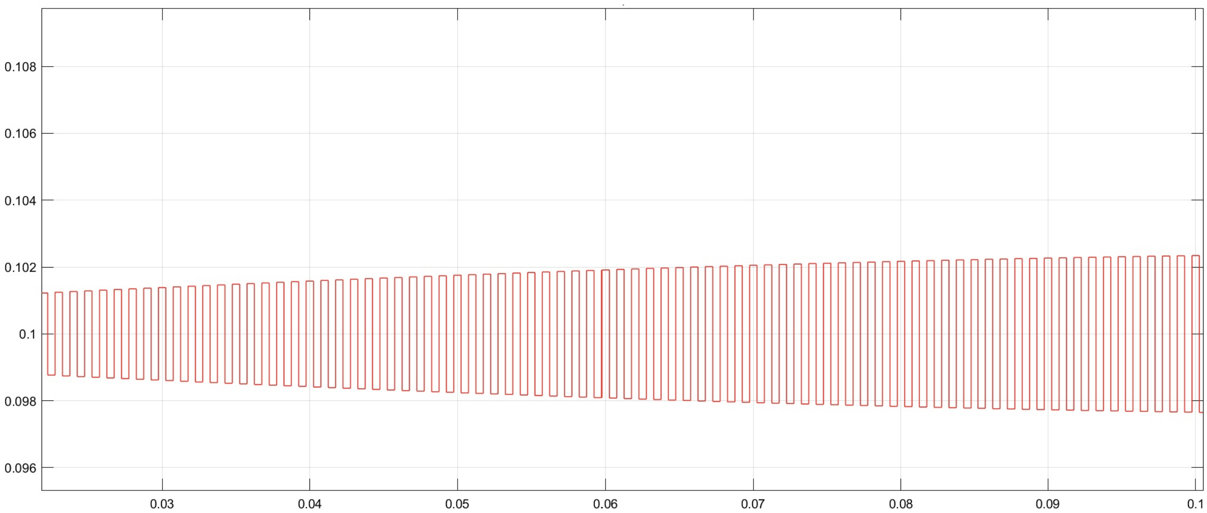

Figure 4.3: Error while using double sample and hold method in high speed

4.1.2 Treatment for amplitude imbalance

When the specific value of amplitude cannot be known, some operations can be used to make the error between the actual amplitude value and the actual amplitude value smaller.

$$V_{sin} = A\sin(\theta) \tag{4.4}$$

$$A\sin(\theta)\sin(\theta') + \cos(\theta')\cos(\theta') = (A-1)\sin(\theta)\sin(\theta') + 1 \tag{4.5}$$

The value of equation (4.5) is within the limit [1,A] if A is more than 1, so when the two equations are divided, the error will be reduced so that the amplitude of the input sine signal of the ATO remains around 1.

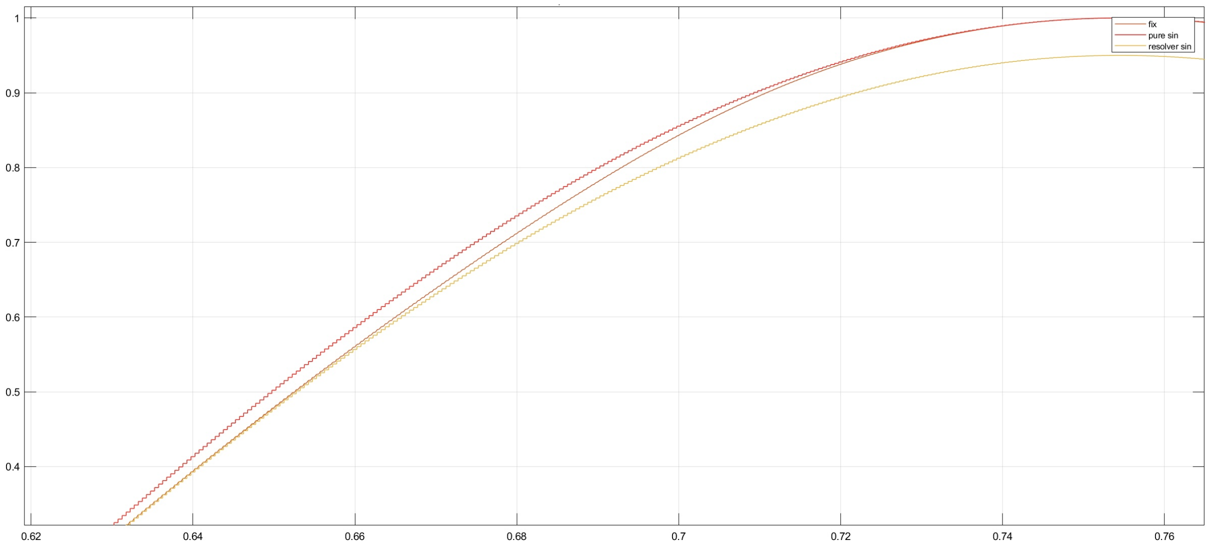

Figure 4.4: Treatment for amplitude imbalance

4.2 Improvement combined with the ATO

The improvement is added before the resolver signals is being inputted into the ATO. With the influence of the DC offset and the amplitude imbalance being removed, The results will look like shown in the figure 4.5.

It is evident from the data that the results are sufficient in accuracy and that the inaccuracy increases to 2.5 degrees only during transitions. However, there is a 0.02 second initial delay in the ATO that also happens during transitions.

4.3 KF added to the feedback of ATO

As shown in the earlier sections that the kalman filter itself is a fast estimator of the state and causes noteably less delays, addition of kalman filter to the model could be a solution. When the Kalman Filter is added to the feedback of the ATO, the initial delay can be reduced by half and the delay during transitions can be completely eliminated. The results of RDC with the kalman filter added to the feedback of the ATO is shown in figure 4.6.

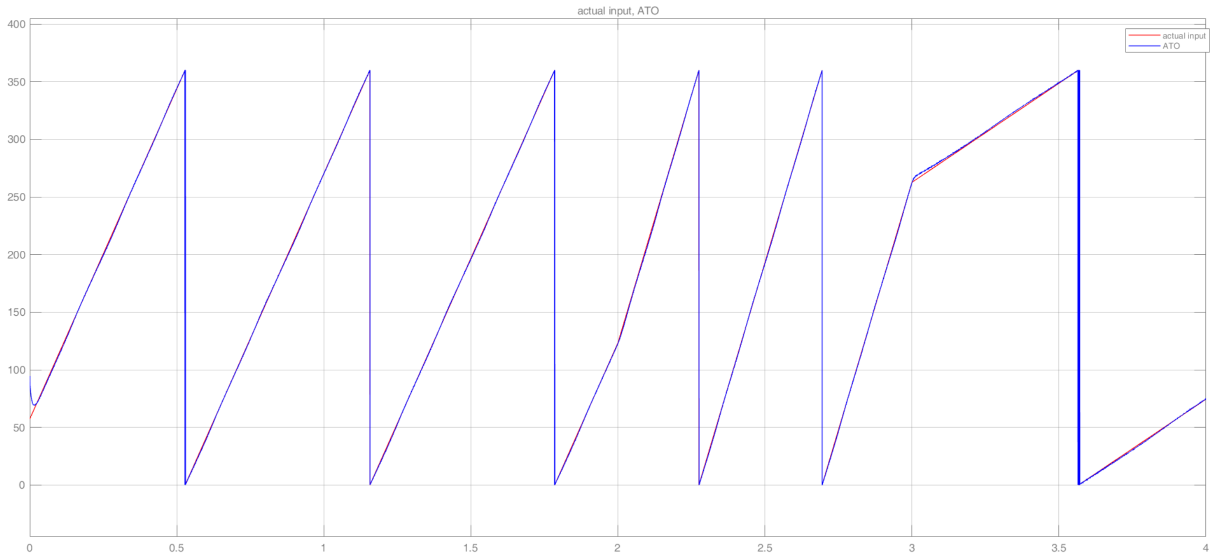

Figure 4.5: Results of the RDC with ATO combined with the added improvements

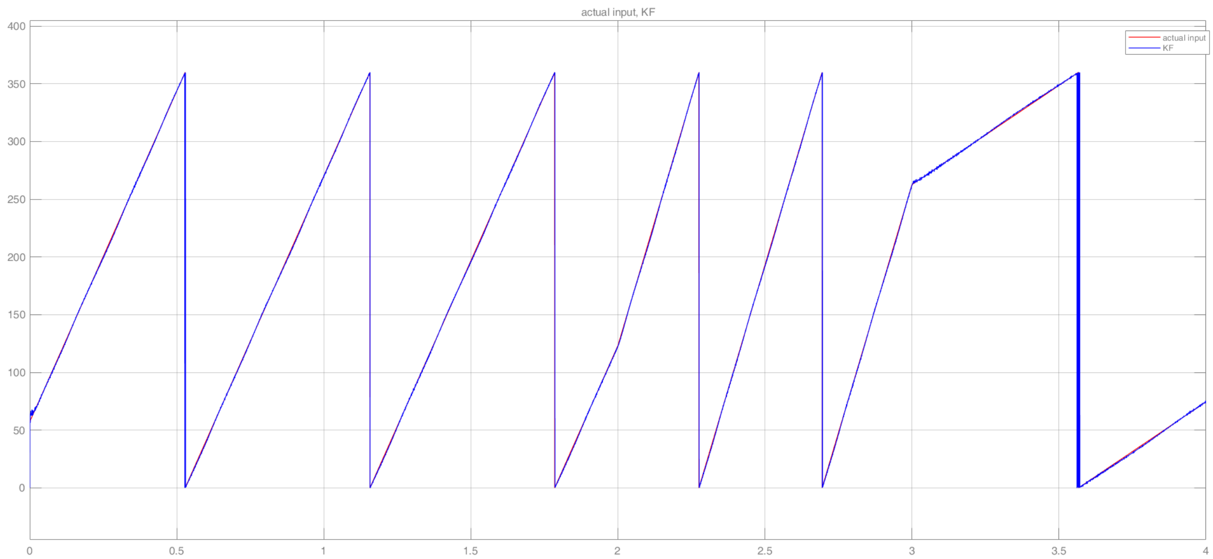

Figure 4.6: Results of the RDC with KF added to the feedback

It can be clearly seen from the results that there is very less delay in the initial stages of encoding and no delay at all during transitions. With an error of a maximum of 1.5 degrees throughout, the kalman filter added to the feedback of the ATO combined with the amplitude imbalance and DC offset treatment methods will be an optimal solution for the resolver's RDC.

All four of the faults in question are treated by the aforementioned method. As not all mistakes are present constantly, it is now necessary to combine the errors to see how the algorithm responds to the various sizes of errors. By controlling the phase error from the phase detector, which is dependent on the property of perpendicular symmetry in the resolver outputs, Phase Locked Loop(PLL) in the PIC can detect the measured angle [4]. It is not intermingled with the other inaccuracies to investigate because the phase shift is always automatically regulated and the error is already eliminated.

The algorithm can deal with a severe amplitude imbalance value of 0.95 and a DC offset value even as high as 1. As our final core algorithm uses a kalman filter, which has noise associated with it, adjusting the noise values reveals that the results are negatively impacted by adding values for noise with sample times shorter than 1/frequency (extremely high frequency noise). The ATO technique stated in section 4.2 is able to tolerate even greater noise levels, even if the KF can only handle high frequency noises up to the specified sample time. Overall, the approach appears promising when simulated with the different inaccuracies and can also handle extremities.

5 Conclusion

5.1 Summary

Various RDC methods have been researched and repeated throughout the study. The software programs utilized throughout the research were Matlab and Simulink. Over 30 percent of our initial work was spent understanding how the resolver worked and modeling it using a literature review. The reproduced academic works were then used to better understand the model's operation and to discover how transitions affect it in Simulink. The errors which were added to the resolver made were unreasonably high in order to learn how the models work under extremities. The benefits and drawbacks of various RDC approaches have then been stated for a method combination. Later, techniques for eliminating amplitude imbalance and DC offset were developed in light of the fact that they had the greatest impact on the output of the RDC. The ATO is then used to encode angles using the processed signals. Even if the ATO alone appears to be dependable, the time delay between the beginning and transitional phases as well as the potential for accumulative errors were causes for worry. But to overcome the flaw, the kalman filter—a precise and speedy estimator of the state was added to the ATO's feedback. The KF added to the ATO's feedback has a maximum inaccuracy of 1.5 degrees on the amplitude imbalance and DC offset treated signals, which is pretty little when you consider how the resolver sensor works. Since our application involves non-linear systems, the aforementioned approach is thus regarded to be the optimal one.

5.2 Future work

The tuning of the noise matrices of the kalman filter and the ATO gain constants is carried out by trial and error method in this project and hence the time consumption is quite high. The time needed to choose such constant values can be reduced by using auto tuning software for both ATO and KF. Since PI controllers are among the most frequently used closed-loop controllers in the market, using machine learning techniques like generic algorithms to tune the PI controller would ultimately provide a PI controller that is almost flawless. Also for the Kalman filter as tuning is an issue, a clever answer to this issue is reinforcement learning, which creates a set of ideal parameters by combining dynamic programming with exploratory testing. More complexity can be added to the developed kalman filter method to improve the state estimation's accuracy. Making use of analytical methods can be robust but the computation power required might be a concern. For this, a resolver angle tracking method based on artificial neural networks(ANN), such as that described in [20] or deep neural networks(DNN) as in the study [21], could provide a solution.

5.3 Ethics and Environment

The information obtained by the sensor 'resolver' is the speed and position of the rotor, and does not contain information about the driver, passengers or pedestrians on the road, so it does not affect the privacy of relevant personnel; due to the reduction of sensor errors, its accuracy is improved, which means the maneuverability of the car has been enhanced, and the safety of the driver and associated road users has also been improved.

Due to the error of the sensor 'resolver' can be controlled within two degrees, the on-board ECU can make an improvement on controlling the output of the motor, which elevates the handling of the vehicle, more efficient control means less energy wastage. Whether it is the improvement of system control accuracy or the improvement of energy transmission efficiency by using an optimized sensor, as one of the important electronic component sensors of electric vehicles, the optimization of the sensor will enhance the user's driving experience, thus affecting the user's decision to choose a traditional internal combustion engine vehicle or an electric vehicle, thereby obtaining better sales in EV/HEV and reducing carbon dioxide and other greenhouse gas emissions.

Bibliography

[1] Q. A. Tianpei Li and G. Rizzoni, "Motor resolver fault propagation analysis for electrified powertrain," October 2017.

[2] Y. Y. Z. W. Fangzhou Wang, Tingna Shi and C. Xia, "Resolver-to-digital conversion based on acceleration-compensated angle tracking observer," vol. 68, October 2019.

[3] Y. H. Kim and S. Kim, "Software resolver-to-digital converter for compensation of amplitude imbalances using d-q transformation," vol. 8, 2013.

[4] H. Qin and Z. Wu, "Angle tracking observer with improved accuracy for resolver-to-digital conversion," 1 November 2019.

[5] M. Guo and Z. Wu, "Noise reduction for high-accuracy automatic calibration of resolver signals via dwt-svd based filter," 9 May 2019.

[6] L. Harnefors, "Speed estimation from noisy resolver signals," 1996.

[7] C. Datlinger and M. Hirz, "Investigations of rotor shaft position sensor signal processing in electric drive train systems," June 2018.

[8] M. Benammar and A. Gonzales, "A novel pll resolver angle position indicator," vol. 65, Jan. 2016.

[9] D. C. L. Pecly, R. Schindeler and K. Hashtrudi-Zaad, "High precision resolver-to-velocity converter," vol. 66, Nov. 2017.

[10] Z. Z. Wang and Z. Zuo, "A novel design method for resolver to-digital conversion," vol. 62, Jun. 2015.

[11] K. Wang and Z. Wu, "Hardware-based synchronous envelope detection strategy for resolver supplied with external excitation generator," vol. 7, Feb. 2019.

[12] M.-H. Kim and D.-Y. Kim, "Accuracy improvement in resolver offset detection based on angle tracking observer with coordinate transformation," 10 July 2021.

[13] O. W. Seta Yuliawan and N. Setiawan, "Kalman filter to improve performance of pid control systems on dc motors," vol. 5, September 2021.

[14] C. M. R. Sivappagari and N. R. Konduru, "High accuracy resolver to digital converter based on modified angle tracking observer method," vol. 144, September 2012.

[15] R. Hoseinnezhad and P. Harding, "A novel hybrid angle tracking observer for resolver to digital conversion," December 2005.

[16] R. van de Schoot; Sarah Depaoli; Ruth King; Bianca Kramer; Kaspar Märtens; Mahlet G. Tadesse; Marina Vannucci; Andrew Gelman; Duco Veen; Joukje Willemsen; Christopher Yau, "Bayesian statistics and modelling," January 2021.

[17] M. I. Ribeiro, "Gaussian probability density functions: Properties and error characterization," February 2004.

[18] B. Anderson and J. Moore, "Optimal filtering," 1979.
[19] G. H. Martin A. Skoglund and D. Axehill, "Extended kalman filter modifications based on an optimization view point."
[20] R. Celikel, "Ann based angle tracking technique for shaft resolver," 5 August 2019.
[21] M. K. M. Emadaleslami and Z. Nasiri-Gheidari, "A high-accuracy two-stage deep learning-based resolver to digital converter," 3 February 2022.